

# SARAF BEAM COMMISSIONING RESULTS: INJECTOR, MEBT

J. Dumas<sup>†</sup>, A. Chance, D. Chirpaz, D. Darde, G. Desmarchelier, R. Duperrier, G. Ferrand, A. Gaget, F. Gohier, F. Gougnaud, T. Joannem, V. Nadot, N. Pichoff, F. Senee, C. Simon, N. Solenne, D. Uriot, L. Zhao

Commissariat à l'énergie atomique et aux énergies alternatives, Gif-Sur-Yvette, France

S. Cohen, H. Isakov, I. Gertz, N. Goldberger, B. Kaizer, A. Kreisel, Y. Luner, I. Mardor, H. Paami, A. Perry, I. Polikarpov, E. Reinfeld, J. Rodnizki, A. Shor, I. Shmueli, Y. Solomon, N. Tamim, R. Weiss-Babai, L. Weissman, T. Zchut, Soreq Nuclear Research Center, Yavne, Israel

## Abstract

IAEC/SNRC in Israel is in the process of constructing a neutron production accelerator facility called SARAF. The facility will utilize a linac to accelerate a 5 mA CW deuteron and proton beam up to 40 MeV. In the first phase of the project, IAEC completed construction and operation of a linac (referred to as SARAF Phase I) which included an ECR ion source, a Low-Energy Beam Transport (LEBT) line, and a 4-rod RFQ. The second phase of the project involves collaboration between IAEC and CEA in France to manufacture the linac. Recently, the injector control system has been updated and the Medium Energy Beam Transport (MEBT) line has been installed and integrated into the infrastructure. Testing and partial commissioning of the injector and MEBT were completed in 2022, and this paper presents the results of that work prior to the delivery of the cryomodules.

## INTRODUCTION

The Medium Energy Beam Transport (MEBT) section spans approximately 5 meters and consists of 3 rebunchers and 8 quadrupoles, each equipped with a steerer for orbit correction. The MEBT serves various purposes, including adapting the beam from the RFQ to the Linac, cleaning the transverse halo (if necessary) using three sets of slits and a chopper (which will be installed later on), minimizing the residual gas sent to the Superconducting Linac (SCL), and characterizing beam properties such as current, position, phase, energy, transverse and longitudinal profiles, and emittances. The MEBT was initially constructed and tested at CEA Saclay during the first half of 2020. A dedicated test stand was utilized to ensure proper alignment, vacuum, cooling, power supplies, and associated control systems. Subsequently, the MEBT was transported to Israel in August 2020 to be installed and integrated by SNRC teams in its final position between the RFQ and a D-plate that was previously employed during Phase I. The MEBT was commissioned in two phases with beam at SNRC, with the first in December 2021 and the second from May-December 2022, conducted in parallel with other activities. All available diagnostics for the commissioning phase are displayed in Figure 1, including two ACCTs for current monitoring, transmission, and SBCT, four BPMs for measuring beam

position and phase, one Fast Faraday Cup (FFC) in the first diagnostic box, and one Faraday Cup at MEBT exit in the second diagnostic box. These diagnostics were primarily used to measure beam transmission, provide protection, and facilitate longitudinal characterization. A wire scanner in the first diagnostic box and a SEM-Grid in the second diagnostic box were later installed during the second semester of 2022 for transverse characterization.

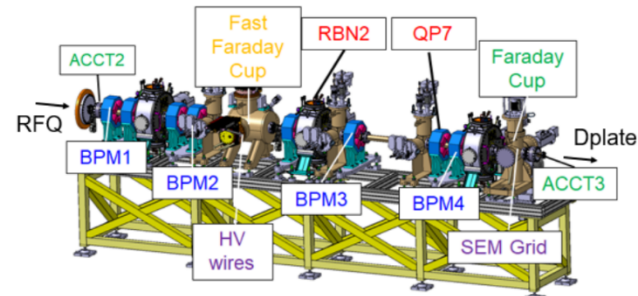


Figure 1: diagnostics and layout of the MEBT the 8 quadrupoles are in blue and red and the 3 rebunchers are in light grey.

After ACCT3, a D-plate was connected, and Figure 2 shows available diagnostics for longitudinal characterization, such as phase probes, FFC, FC and MPCT for current monitoring and a set of slits and wires for transverse emittance measurements.

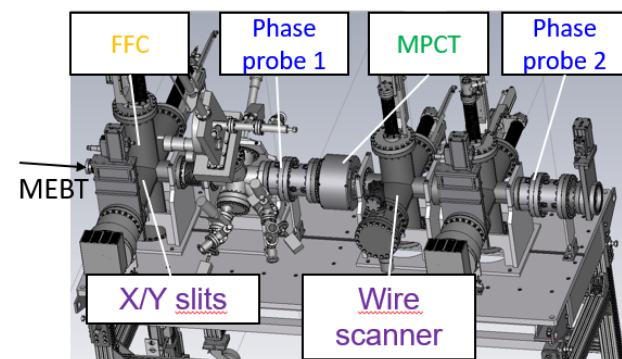


Figure 2: available D-plate diagnostics [1]

A temporary beam line with two transverse profilers and two FC stations, as well as the Galium Indium Liquid Target (GALIT) was installed downstream for high duty cycle operation.

<sup>†</sup>jonathan.dumas@cea.fr

## COMMISSIONING WITH BEAM

### RFQ and MEBT Transmission Measurements

Using the new LLRF hardware and software [2], the required voltages for proton operation were applied to the RFQ and rebunchers. The LEBT optics were adjusted to maximize beam transmission at the RFQ exit. Beam current was measured at different locations, including the LEBT ACCT1, ACCT2 immediately after the RFQ exit, and FC at the end of the MEBT. Figure 3 shows that the transmission plateaus at 710 mV (over 90%), which is the most efficient voltage from a transmission perspective. The RFQ transmission obtained in this phase is significantly higher than what was reported in Phase I [3]. The reason for this discrepancy is unclear and may be attributed to improvements made to the SARAF ion source at this stage. To determine the transmission through the full MEBT, the beam was stopped at the FC, and the current measured there and in the ACCT2 was compared with the one measured in ACCT1 (before the RFQ). The MEBT optics were adjusted based on beam dynamics simulations for this specific measurement. The measurements demonstrated almost 100% MEBT transmission.

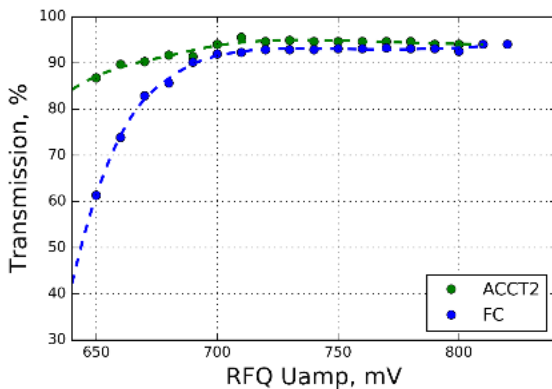


Figure 3: Beam transmission in ACCT2, in green, and the FC, in blue, of the MEBT as a function of the LLRF Uamp (RFQ voltage).

### Rebuncher Phasing

The two BPMs located after each cavity serve as phase probes to tune the three rebunchers using the Signature Matching method [4]. The data obtained from the measurement was well-matched with a cosine fit and TraceWin simulations. However, there was a difference between the rebuncher phase of no acceleration and the average estimated energy phase from the fit, resulting in a  $12^\circ$  offset between the two points (as shown in Figure 4). This discrepancy was observed for all the rebunchers. It is due to a poor compensation of the beam loading and disappears with a better setting of the LLRF. For the third rebuncher, phase probes from the D-plates were used.

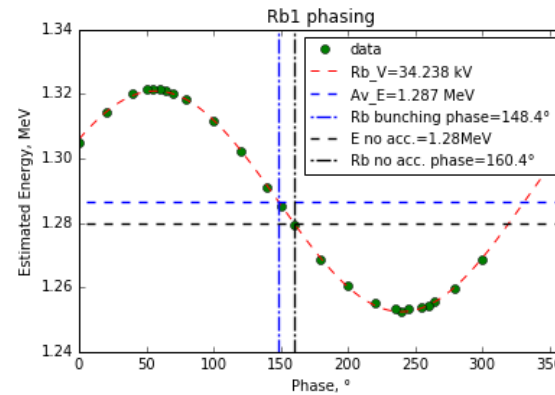


Figure 4: Rebuncher 1 phasing. In green is the estimated energy based on the measurement of the phase difference between BPM2 and 3. In red is the cosine fit. In black and blue are the discrepancy between the phase of no acceleration and the phase of the fit energy average.

### Bunch Longitudinal Size Measurement

The Fast Faraday Cup, which is located after the first rebuncher, is used to measure the longitudinal bunch profile. The measured profile is found to be in good agreement with the expected profile from simulations, as illustrated in Figure 5. Nevertheless, applying appropriate filters to mitigate noise or negative bouncing (at  $50^\circ$  for example) in the experimental waveform can lead to further improvements in the accuracy of the measured profile.

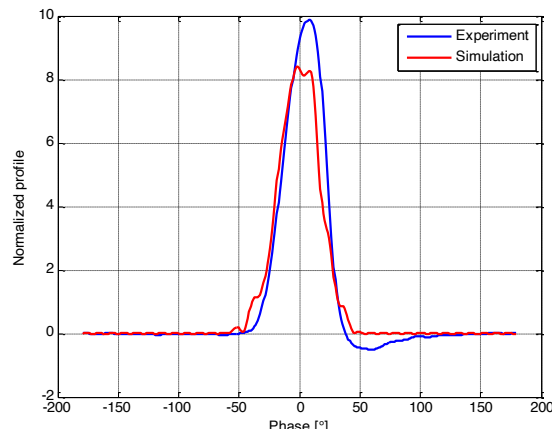


Figure 5: bunch longitudinal profile measured on the FFC after the first rebuncher in blue, and the TraceWin simulation in red.

### Longitudinal Emittance

The gradient variation method [5] was used to compute the longitudinal emittance. To monitor the bunch length, the rebuncher voltage was varied while the beam was measured at the MEBT FFC, as shown in Figure 6. For this measurement, a low-noise 6 GHz bandwidth amplifier and a 4 GHz scope with fast response were used. To minimize the loss in the long cables, the scope was located close to the FFC.

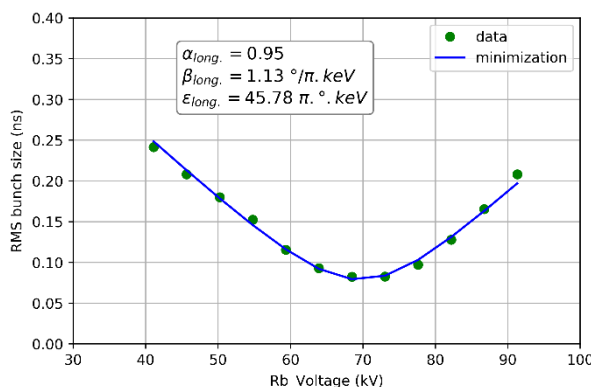


Figure 6: Longitudinal bunch size measured on the FFC as a function of the rebuncher 1 voltage.

### Transverse Emittance

For transverse emittance, the bunch size was measured with the MEBT wire scanner as a function of a quadrupole strength. The Twiss parameters are also computed for the exit of the RFQ, see Figure 7.

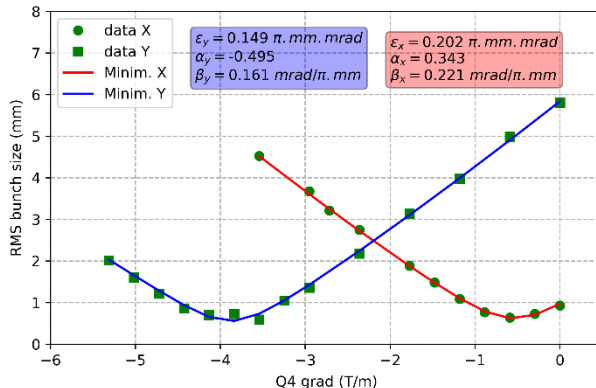


Figure 7: calculated transverse Twiss parameters at the exit of the RFQ from measured wire scanner data in red for the horizontal and blue for the vertical plane.

The transverse emittance is also measured in the Dplate with a set of slits coupled with wires. It allows to construct the phase space presented on Figure 8. The horizontal emittance between the two measurements are consistent. The vertical emittances show a discrepancy of 30% which might be the systematic errors of the measurements.

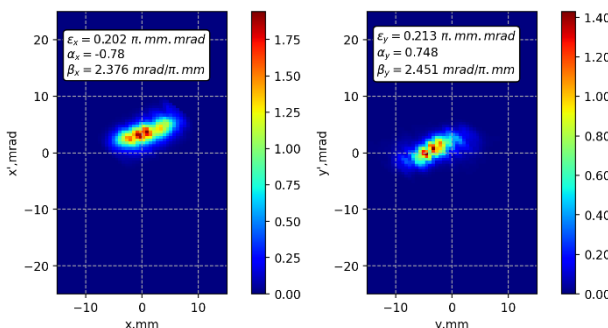


Figure 8: calculated transverse Twiss parameters at the exit of the MEBT from the emittance meter in the DPlate.

### High Power Beam Test

After a first beam power ramp up with a duty cycle of 40% on the MEBT FC. The pulse length was increased to 99ms with a repetition rate of 10Hz on March 23, 2023 to the GALIT. The beam trips from the MPS represented in blue on Figure 9 are a result of beam instability from the RF of the RFQ and still require some investigation in order to reach higher availability. Figure 10 shows the beam current measurement in the Dplate for 50 and 99% duty cycle.

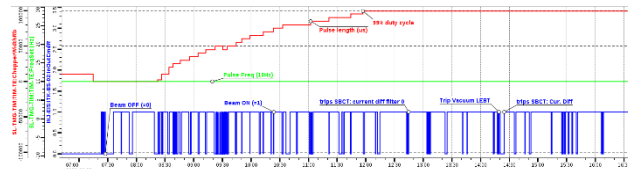


Figure 9: ramping up of duty cycle for a proton beam in the MEBT. Pulse length in red (in  $\mu$ s), pulse frequency in green (in Hz) and beam presence in the beamline in blue.



Figure 10: Current monitoring for 50% duty cycle on the left and 99% on the right with an ACCT installed upstream of GALIT.

### CONCLUSION

The MEBT was installed at SARAF, followed by its commissioning with and without beam. The feasibility of transporting a proton beam of 5 mA average current was demonstrated and the main characteristics were analysed. The commissioning will continue with the transport and characterization of the deuteron beam, and finally the installation and commissioning of the cryomodules.

### REFERENCES

- [1] C. Piel *et al.*, “Phase 1 Commissioning Status of the 40 MeV Proton/Deuteron Accelerator SARAF”, in *Proc of EPAC'08*, Genoa, THPP038, p.3452, June 2008.
- [2] Orolia, <https://orolia.com>
- [3] L. Weissman *et al.*, “Installation, high-power conditioning and beam commissioning of the upgraded SARAF 4-rods RFQ”, *JINST* 13 T05004, May 2018.
- [4] T.L. Owens *et al.*, “Phase scan signature matching for LINAC tuning”, in *Proc. of LINAC 94*, pp. 893- 895, TH-80, august 1994.
- [5] P. Strehl, *Beam Instrumentation and Diagnostics*, Berlin, Springer, 2006